Astron. Astrophys. 317, L5–L8 (1997)

ASTRONOMY
AND
ASTROPHYSICS

LETTER

Letter to the Editor

Spectroscopic evidence of mass infall towards an embedded infrared source in the globule DC 303.8-14.2

K. Lehtinen

Observatory, University of Helsinki, Tähtitorninmäki, P.O. Box 14, FIN-00014 Helsinki, Finland

Received 12 July 1996 / Accepted 20 August 1996

Abstract. We present millimeter molecular line observations towards the embedded infrared source IRAS 13036-7644, located in the globule DC 303.8-14.2. The CS(J=2–1) lines show asymmetrical profiles characteristic of a cloud undergoing gravitational collapse, i.e. double-peaked profiles with a brighter blue-shifted component. In contrast the HCO^+(J=1–0) line shows towards the IRAS source a double-peaked profile with a brighter red-shifted component, and a velocity gradient across the cloud. The hyperfine components of HCN(J=1–0) transition show both kinds of double-peaked profiles, and a velocity gradient. We interpret these results as a simultaneous infall of the dense gas in the core and a non-collapsing envelope.

The IRAS source drives a bipolar molecular outflow detected in the ^{12}CO(J=1–0) transition.

Key words: Line: profiles – Stars: formation – ISM: clouds – ISM: individual objects: DC 303.8-14.2 – ISM: individual objects: IRAS 13036-7644 – ISM: jets and outflows

1. Introduction

Bok & Reilly (1947) and Bok (1948) were the first to suggest that the small, isolated dark clouds called Bok globules are the birthplaces of low mass stars. Infrared observations made by the IRAS have revealed embedded sources, probably young stellar objects (YSOs), inside these clouds (Yun & Clemens 1990; Clemens et al. 1991). Some of these sources drive a molecular outflow (Yun & Clemens 1992), confirming star-forming activity in globules.

In order to identify a true protostar located in a cloud core, it is necessary to have kinematic evidence of mass infall. This is best accomplished through high spatial and spectral resolution molecular line observations. One of the best candidates for a collapsing protostar is located in the globule B335 (Frerking et al. 1987; Zhou et al. 1990; Zhou et al. 1993; Choi et al. 1995; Zhou 1995).

By comparing the properties of globules with and without star formation one can study the processes that lead to star formation in molecular clouds. Lehtinen et al. (1995) have studied a globule without any signs of star formation, the Thumbprint Nebula (TPN) in the Chamaeleon III region. In order to study the properties of molecular gas in a star forming globule, we observed the globule DC 303.8-14.2 (Hartley et al. 1986), located in the eastern part of the Chamaeleon II dark cloud complex, which is at a distance of 200 pc (Whittet et al. 1991; Hughes & Hartigan 1992). It is of a similar size and appearance as the TPN but it harbours an IRAS point source (IRAS 13036-7644, $\alpha(1950) = 13^{\rm h}3^{\rm m}41.4^{\rm s}$, $\delta(1950) = -76^\circ44'3''$) with a spectral energy distribution typical for a young stellar object.

In this Letter we present the first results of our extensive molecular line study of DC 303.8-14.2. We discuss the observed line profiles which display the signature of mass infall towards the IRAS source.

2. Observations

Molecular line observations at 3 and 1.3 mm were made during December 26–27 th 1993 with the 15 m SEST (Swedish ESO Submillimeter Telescope) on La Silla, Chile. The telescope and its instrumentation have been described by Booth et al. (1989). At 3 mm we used a dual polarization Schottky receiver, while at 1.3 mm a single polarization SIS-receiver was used. The telescope half power beamwidth (FWHM) is 57″, 45″ and 23″ at 86, 115 and 230 GHz, respectively.

The spectrometer was a 2000 channel acousto-optical spectrometer, with 43 kHz channel separation and 80 kHz resolution. The channel separation corresponds to $\sim$ 0.14 and

0.05 km s^{-1} at 3 and 1.3 mm, respectively. Pointing was checked by observing SiO masers and it was found to be better than 5″.

The calibration of the antenna temperatures was obtained using the chopper-wheel calibration (Ulich & Haas 1976). The intensities of the observed lines are presented in the $T_{\rm A}^{\star}$ scale.

3. Spectral signatures of a collapsing cloud

There are several theoretical studies of line formation in dense cores undergoing collapse (e.g. Leung & Brown 1977; Leung 1978; Walker et al. 1986; Adelson & Leung 1988; Zhou 1992; Zhou et al. 1993; Walker et al. 1994; Myers et al. 1995; Zhou 1995; Choi et al. 1995). The general results of these studies applied to an emergent line profile from a spherically symmetric cloud with mass infall in the radial direction and an excitation temperature which is increasing inwards, are the following: (1) As the optical depth increases, the line profile progresses from a symmetric single-peaked profile to a double-peaked profile with the blue-shifted component being the brighter. This structure is caused by a self-absorption dip at the centre of the profile. At intermediate optical depths this dip is not pronounced and the profile remains single-peaked but is skewed to blue-shifted velocities. (2) The degree of self-absorption and asymmetry is greatest at the cloud center, and decreases outward. (3) In the case of an expanding cloud a similar sequence of line profiles is obtained with increasing optical depth but in this case the line profile is skewed to red-shifted velocities. (4) Rotation can also produce asymmetric line profiles. However, contrary to the cases with radial movements, the profiles are mirror images of each other relative to the rotation axis. Along the line of sight towards the cloud center, the rotation has no effect and the profiles are symmetric.

A line profile with a brighter red-shifted component is, hereafter said, to have "anti-infall" asymmetry, whether or not this asymmetry is due to expansion.

4. Line profiles

In Fig. 1 we show some of the observed lines towards the IRAS source. The ^{12}CO(J=1–0), HCO$^+$(J=1–0) and CS(J=2–1) lines show a two-peaked profile with either the blue- or red-shifted peak being the brighter whilst the other lines show a single-peaked profile. The peaks of the rarer isotopes coincide with the dip of the main isotopic lines. Thus, the dips in these profiles are not due to two clouds at different radial velocities but are rather caused by absorption in a foreground material with a lower excitation temperature.

In addition to the lines presented here, the CS(J=3–2) and $H_2CO(2_{12}–1_{11})$ profiles are double-peaked with the blue-shifted component being the brighter, and the DCO$^+$(J=1–0) line is skewed towards blue. A detailed modelling of all the line profiles is being undertaken using a non-LTE radiative transfer program (Lehtinen et al. 1996, in preparation).

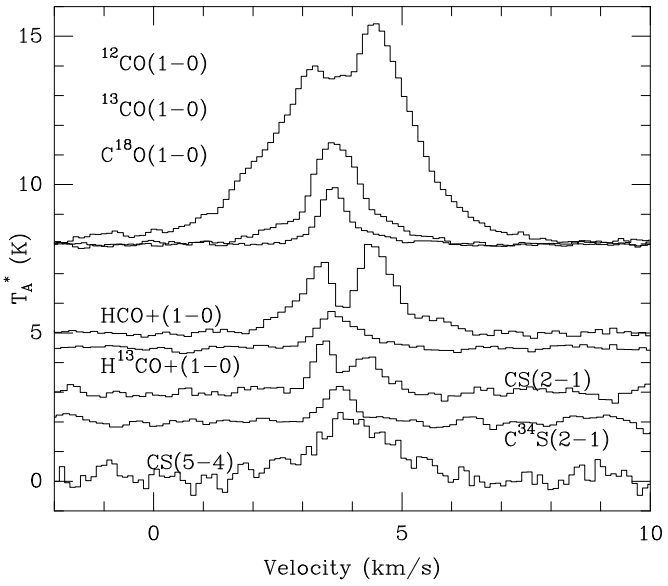

Fig. 1. Some of the observed lines towards the IRAS source. The lines are from top to bottom: ^{12}CO(J=1-0), ^{13}CO(J=1-0), 2×C^{18}O(J=1-0), HCO$^+$(J=1-0), 2×H^{13}CO$^+$(J=1-0), 2×CS(J=2-1), 8×C^{34}S(J=2-1) and 8×CS(J=5-4)

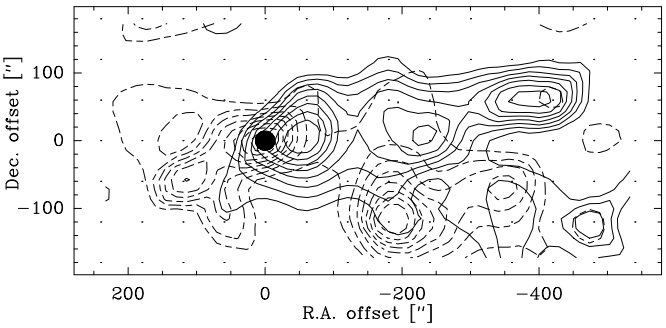

Fig. 2. A map of the integrated intensity of ^{12}CO($J = 1 - 0$) emission over the velocity intervals 0–1 (solid contours) and 6–7 km s^{-1} (dashed contours). The contours are from 0.1 to 0.8 in steps of 0.1 K km s^{-1}. The IRAS source is marked with a black circle

4.1. ^{12}CO(J=1–0)

The ^{12}CO($J = 1 - 0$) line profiles show broad wings extending from -2 to +8 km s^{-1}. In Fig. 2 we show the velocity integrated line maps over the velocity intervals 0–1 (solid contours) and 6–7 km s^{-1} (dashed contours). The IRAS source at (0,0) drives an outflow, which is oriented approximately in the east-west direction. The outflow is more extended to the west than to the east. At the position ($\Delta\alpha, \Delta\delta$)=(-200″, -100″) there is indication of another red-shifted outflow component.

4.2. CS(J=2–1) and CS(J=5–4)

The central part of the observed CS(J=2–1) map is shown in Fig. 3. The spectra on and near the IRAS position at (0,0) show

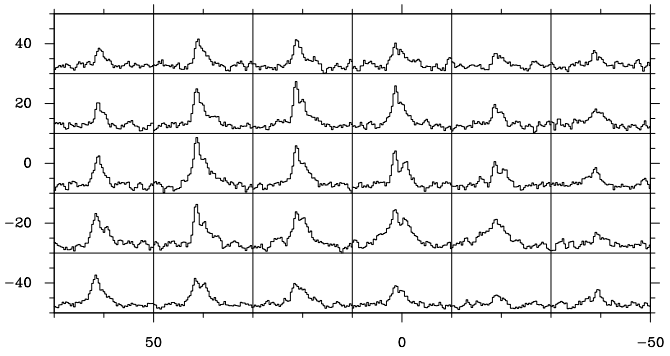

Fig. 3. The central part of the observed CS(J=2-1) spectral line map. The offsets are in units of arc-seconds. The velocity axis extends from 0.0 to 8.0 km s^{-1}, and the antenna temperature extends from -0.2 to 1.3 K

a double-peaked profile with the blue-shifted peak brighter than the red one while further away the lines are single-peaked but skewed towards the blue. This behaviour is just what is expected for a collapsing cloud. The symmetric shape of the J=5–4 transition can be explained if it is optically thin. The J=5–4 transition is wider than the J=2–1 transition, as predicted by infall models (Zhou 1992).

4.3. HCO$^+$(J=1–0)

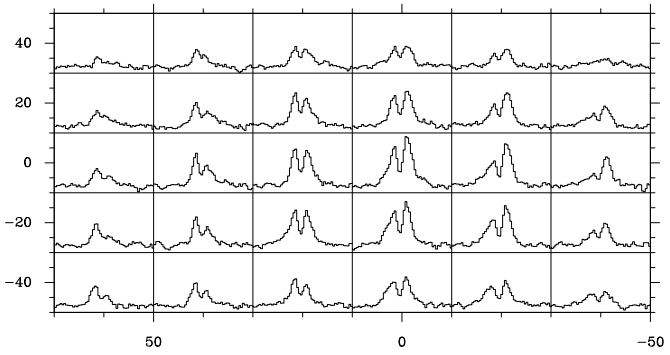

Fig. 4. A map of the HCO$^+$(J=1–0) profiles. The offsets are in units of arc-seconds. The velocity axis extends from 0.0 to 8.0 km s^{-1}, and the antenna temperature extends from -0.4 to 3.2 K

In Fig. 4 a map of the HCO$^+$(J=1–0) emission is shown. There is a symmetry axis, approximately in the north-south direction at $\Delta\alpha \approx 20''$. There is a reversal of line profiles east and west of this symmetry axis in the sense that the left-hand line component is stronger on the eastern and the right-hand component on the western side. This kind of asymmetry in the profiles is just what is expexted for a rotating cloud, with the symmetry axis as the axis of rotation (Adelson & Leung 1988). Thus the cloud DC 303.8-14.2 would have a rotation axis oriented in the north-south direction. Another possible cause for the observed velocity gradient is the outflow, which is also oriented in the east-west direction.

If the asymmetry in the line profiles were due to rotation only, then along the lines of sight towards the rotation axis the line profiles would not be affected by the cloud rotation. If the rotation axis were located at $\Delta\alpha$ = 0, the observed profiles (higher red- than blue-shifted component) at $\Delta\alpha$ = 0 would indicate that there is radial expansion of the mass traced by HCO$^+$ emission. This would be the opposite as determined from the CS profiles. However, without a detailed knowledge of the cloud structure, other explanations for the asymmetrical profiles, e.g. deviation of low density material from spherical symmetry, or an uneven contribution from red-shifted and blue-shifted outflow emission, can not be ruled out.

There are two problems which complicate the interpretation of the HCO$^+$ profiles. Firstly, what is the real position of the IRAS source ? The IRAS Point Source Catalog gives for the positional error ellipse the semi-major and semi-minor axes of $20''$ and $6''$, respectively. The position angle from north to east of the major axis is 15°. If the IRAS source were located at $\Delta\alpha \approx 20''$ to the east, the HCO$^+$ profiles would be symmetric towards it. This is, however, improbable given the positional uncertainty of the IRAS source. Secondly, is the IRAS source located at the center of the cloud, i.e. is it located on the possible rotation axis ? This would be expected if the star was very recently formed. On the other hand, if the star had a projected velocity of 1.0 km s^{-1} (Clark 1987), it would take $\sim 2.0 \times 10^4$ yrs to travel an angular distance of $20''$. In comparison, the maximum ages of Class 0 and Class I objects are estimated to be $\sim 10^4$ and $\sim 10^5$ yrs, respectively (André 1994).

4.4. HCN(J=1–0)

In Fig. 5 we show HCN(J=1–0) spectra at the IRAS source position (0,0) and $20''$ east and west of it. Each one of the three hyperfine structure (hfs) components is seen to display the two velocity peaks seen in CS(J=2–1) and HCO$^+$(J=1–0) lines. In LTE, the optical thicknesses of the hfs components have the ratios 1:5:3 (F=0–1:F=2–1:F=1–1, from left to right). The observed line intensities are more equal, however, indicating substantial optical depths. The central and the rightmost hfs components, with the highest optical depths, have a behaviour similar to the HCO$^+$(J=1–0) line, i.e. at the (0,0) position the red-shifted peak is higher than the blue-shifted one, and at the eastern position the profiles are reversed. On the other hand, the leftmost hfs component, with the lowest optical depth, behaves similarly to the CS(J=2–1) line, i.e. the blue-shifted peak is the stronger one.

5. Discussion

The CS(J=2–1) and HCN(J=1–0, F=0–1) line profiles indicate mass infall towards IRAS 13036-7644. However, a determination of excitation conditions as a function of the cloud radius is necessary before a unique interpretation of the observed line profiles can be given.

However, the ^{12}CO(J=1–0), HCO$^+$(J=1–0) and HCN(J=1–0, F=2–1/1–1) line profiles towards the IRAS

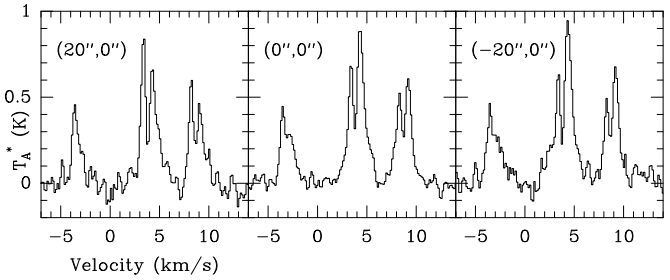

Fig. 5. A cross scan of HCN(J=1–0) spectra across the IRAS source in the east-west direction

source show an "anti-infall" asymmetry. The situation is similar to the HCO^+(J=1–0) profiles in the collapse candidate B335 with "anti-infall" asymmetry observed by Frerking et al. (1987). According to their model of B335 the core is collapsing, but the envelope is expanding due to the magnetic flux enhancement caused by ambipolar diffusion out of the core. This model produces HCO^+(J=1–0) profiles which are consistent with observations. However, the HCO^+(J=3–2) line in B335 shows a profile characteristic of infall (Zhou et al. 1993). It is expected that the J=1–0 transition of HCO^+ traces much less dense gas (i.e. the envelope) than the J=3–2 transition (e.g. Gibb et al. 1994). The shape of the observed line profile (infall or "anti-infall" asymmetry) is determined by optical depth effects (see Leung and Brown 1977; Leung 1978). This behaviour is well demonstrated by our HCN lines.

One should note that the observed line profile in a collapsing cloud is strongly dependent on the angular resolution of the observations (Zhou 1992). The telescope beam has to be small enough compared to the infall region in order to reveal the infall signature. However, the HCO^+(J=1–0) line profile towards the IRAS source would not turn into a profile with infall asymmetry even if observed with a higher angular resolution: the observed HCN(J=1–0) hyperfine components show that both infall and "anti-infall" asymmetry can be seen with the same angular resolution, depending on the optical depth of the transition.

All the lines that trace high density gas are consistent with mass infall towards IRAS 13036-7644. None of the low density gas tracers indicate infall, but some of them show a profile with "anti-infall" asymmetry. Thus the outer parts of the cloud are probably not in a state of collapse. Thorough modelling is required to find out whether the "anti-infall" asymmetry is due to expansion, outflow, or some other reason.

References

Adelson, L.M., Leung, C.M. 1988, MNRAS, 235, 349

André, P. 1994, In *The Cold Universe*, eds. Montmerle, T., Lada, C.J., Mirabel, I.F., Trân Thanh Vân J., pp. 179-192, Gif-sur-Yvette, France: Frontières

Bok, B.J., Reilly, E.F. 1947, ApJ, 105, 255

Bok, B.J. 1948, Centennial Symposia, Harv. Obs. Monogr., 7, 53

Booth, R.S., Delgado, G., Hagström, M., Johansson, L.E.B., Murphy, D.C., Olberg, M., Whyborn, N.D., Greve, A., Hansson, B., Lindström, C.O., Rydberg, A. 1989, A&A, 216, 315

Choi. M., Evans II, N.J., Gregersen E.M., Wang, Y. 1995, ApJ, 448, 742

Clark, F.O. 1987, A&A, 180, L1

Clemens, D.P., Yun, J.L., Heyer, M.H. 1991, ApJS, 75, 877

Frerking, M.A., Langer, W.D., Wilson R.W. 1987, ApJ, 313, 320

Gibb, A.G., Little, L.T., Heaton, B.D., Lehtinen, K.K. 1995, MNRAS, 277, 341

Hartley, M., Manchester, R.N., Smith, R.M., Tritton, S.B., Goss, W.M. 1986, A&AS, 63, 27

Hughes, J., Hartigan, P. 1992, AJ, 104, 680

Lehtinen, K., Mattila, K., Schnur, G.F.O., Prusti, T. 1995, A&A, 295, 487

Leung, C.M., Brown, R.L. 1977, ApJ, 214, L73

Leung, C.M. 1978, ApJ, 225, 427

Myers, P.C., Bachiller, R., Caselli, P., Fuller, G.A., Mardones, D., Tafalla, M., Wilner, D.J. 1995, ApJ, 449, L65

Ulich, B.L., Haas, R.W. 1976, ApJ, 30, 247

Walker, C.K., Lada, C.J., Young, E.T. 1986, ApJ, 309, L47

Walker, C.K., Narayanan, G., Boss, A.P. 1994, ApJ, 431, 767

Whittet, D.C.B, Assendorp, R., Prusti, T., Roth, M., Wesselius, P.R. 1991, A&A, 251, 524

Yun, J.L., Clemens, D.P. 1990, ApJ, 365, L73

Yun, J.L., Clemens, D.P. 1992, ApJ, 385, L21

Zhou, S., Evans II, N.J., Butner, H.M., Kutner, M.L., Leung, C.M., Mundy, L.G. 1990, 363, 168

Zhou, S. 1992, ApJ, 394, 204

Zhou, S., Evans II, N.J., Kömpe, C., Walmsley, C.M. 1993, ApJ, 404, 232

Zhou, S. 1995, ApJ, 442, 685

This article was processed by the author using Springer-Verlag LaTeX A&A style file *L-AA* version 3.